PHYSICAL REVIEW D **80,** 014004 (2009)

Exclusive nonleptonic $B \to VV$ decays

N. Barik,[1,*] Sk. Naimuddin,[2,†] P. C. Dash,[3] and Susmita Kar[4]

[1]*Department of Physics, Utkal University, Bhubaneswar-751004, India*
[2]*Department of Physics, Maharishi College of Natural Law, Bhubaneswar-751007, India*
[3]*Department of Physics, Prananath Autonomous College, Khurda-752057, India*
[4]*Department of Physics, North Orissa University, Baripada-757003, India*

(Received 7 March 2009; published 7 July 2009)

The exclusive two-body nonleptonic $B \to VV$ decays are investigated, within the factorization approximation, in the relativistic independent quark model based on a confining potential in the scalar-vector harmonic form. The branching ratios and the logitudinal polarization fraction (R_L) are calculated yielding the model predictions in agreement with experiment. Our predicted CP-odd fraction ($R_\perp$) for $B \to D^* D^*_{(s)}$ decays are in general agreement with other model predictions and within the existing experimental limit.

DOI: 10.1103/PhysRevD.80.014004 PACS numbers: 12.39.Pn, 13.25.Hw

I. INTRODUCTION

The nonleptonic weak decay of B mesons is important as it provides a good opportunity to probe the interplay of QCD and electroweak interactions, to evaluate the Cabibbo-Kobayashi-Maskawa (CKM) elements like "V_{bc}" and "V_{bu}," and to study the CP violation to find possible hints for any new physics beyond standard model (SM). The mechanism of these decays, however, is still not clear in the SM framework. The problem essentially lies in the calculation of transition amplitude where one needs to evaluate the matrix element of the local four-quark operators in the nonperturbative QCD approach. Various approaches within the factorization approximation [1–5] have been employed to evaluate the transition amplitudes and explain existing data in the $B \to PP$, PV, VV decay channels within the limitation of the method.

If weak annihilation contributions are ignored, the analysis of such decay is simplified by using the factorization hypothesis in which the hadronic matrix element of the local four-quark operators is factorized into two single current matrix elements: one connecting the parent B meson with one of the daughter mesons and the other connecting the vacuum with the second daughter meson. The analysis of two-body nonleptonic weak B decays is thus reduced to the evaluation of the relevant meson form factors parametrizing hadronic matrix elements as in the case of semileptonic decays and the meson decay constants describing the leptonic decays. This makes the factorization hypothesis an appealing assumption for analyzing these decays. Theoretical developments based on the QCD approach in the $\frac{1}{N_c} \to 0$ limit [6], Bjorken's intuitive argument based on color transparency [7], and the heavy quark effective theory [8] have justified the factorization approximation in energetic nonleptonic B decays of $B \to PP$, PV type. In such decays, the strong interaction effects such as the final state interactions and rescattering of final state hadrons, as well as the renormalization point dependence of the initial and factorized amplitudes, have been shown [9] to be marginal. Similar arguments, however, may not hold up well in analyzing $B \to VV$ decays involving two vector mesons in the final state.

In $B \to VV$ decays, the strong interaction effects can not be considered negligible when both the mesons in the final state are heavy and are expected to be in the region close to the zero recoil. Contributions to these decay rates come from both the longitudinal and transverse polarization fractions which can be measured in the experiments. It is also known from the naive counting rules based on the factorization approach that the longitudinal polarization dominates the decay rate and transverse polarization is suppressed. In fact much attention has been paid in the literature to the two-body charmless hadronic B decays, but there has been relatively less discussion on the $B \to VV$ decays with one or both charmed vector mesons in the final state. The two charmed meson decays of B mesons are of special interest as they provide valuable information which is different from the light meson productions. For example, CP asymmetries in $B \to D^{*+} D^{*-}$ play an important role in testing the SM and exploring new physics beyond SM. Moreover, these decays are ideal modes to check the factorization hypothesis, as the phenomenon of color transparency applicable to the light energetic hadrons is not valid in these cases. The recent data from the BABAR and Belle collaboration experiments [10,11] have produced considerable theoretical interest in these decays. Since the decay branching ratios (BRs), CP asymmetries, and the polarization fractions of $B \to D^* D^*$ and $D^* D^*_s$ have been partially observed in the experiments, it is timely to examine the $B \to VV$ decay modes in more detail. In fact these decays have been studied in the past by various models including Bauer-Stech-Wirbel (BSW) [1], the QCD factorization approach [4], the improved

*nbarik@iopb.res.in
†naim@iopb.res.in

Bouckaert-Smoluchowski-Wigner model [12], the relativistic quark model [13], the constituent quark model (CQM) [14], the light front (LF) QCD [15], and the heavy quark symmetry (HQS)[16]. Some of the predictions were found to satisfy the requirement of the heavy quark effective theory [17]. Recent studies by Cheng *et al.* [15], Luo and Rosner [18], Chen *et al.* [19], Datta and O'Donnell [20], and Thomas [21] have predicted $B \to VV$ decays in reasonable agreement with that of the improved Isgur-Scora-Grinstein-Wise (ISGW) model [22] and the experiment.

We have used the factorization hypothesis to analyze successfully $B \to PP$, PV in the relativistic independent quark model (RIQM) based on the confining potential in the scalar-vector harmonic form [23]. The model in its earlier applications has also predicted successfully a wide ranging hadronic phenomena in the light and heavy flavor sector [24,25]. In this paper we would like to extend the applicability of the RIQM model and predict, within factorization approximation, the $B \to VV$ decays with one or both of the charmed vector mesons in the final state in comparison with existing experimental data and other model predictions.

The paper is organized in the following manner. In the following section we provide the general remarks on factorization hypothesis and nonleptonic decay amplitudes. In Sec. III we describe in brief the RIQM-model framework. In Sec. IV we obtain model expressions for the weak form factors and that of the polarized transition amplitudes. We discuss the numerical results in Sec. V. Section VI embodies our summary and conclusion.

II. GENERAL DEFINITIONS AND FACTORIZATION

In the factorization approach, the decay amplitude for the two-body nonleptonic decays $B(\bar{b}q) \to X(q\bar{q}')Y(q_1\bar{q}_2)$ can be approximated by the product of one particle matrix element [1,13,23] such as

$$\langle XY|H_{\rm eff}|B\rangle = \frac{G_F}{\sqrt{2}} V_{q'b}V_{q_1q_2}[a_1(\mu)\langle Y|J^\mu|0\rangle\langle X|J_\mu|B\rangle + a_2(\mu)\langle X|J^\mu|0\rangle\langle Y|J_\mu|B\rangle], \tag{1}$$

where, G_F is the Fermi constant, $V_{q'b}$ and $V_{q_1q_2}$ are CKM-matrix elements, $J_\mu \equiv V_\mu - A_\mu \equiv \bar{q}'\gamma_\mu(1-\gamma^5)b$ is the vector-axial vector current, and $a_1(\mu)$ and $a_2(\mu)$ denote the strength of interaction expressed in terms of the Wilson coefficients as

$$\begin{aligned} a_1(\mu) &= C_1(\mu) + \frac{1}{N_c}C_2(\mu); \\ a_2(\mu) &= C_2(\mu) + \frac{1}{N_c}C_1(\mu), \end{aligned} \tag{2}$$

where N_c is the number of colors ($N_c = 3$).

In the general case, the renormalization point μ dependence of the product of current operator matrix elements do not cancel the μ dependence of $a_{1,2}(\mu)$. Thus nonfactorizable contributions to Eq. (1) must be present in order to make the physical amplitude renormalization scale independent. In the present analysis as in Ref. [21], the nonfactorizable vertex, penguin, and hard spectator corrections are thought to be incorporated into the effective Wilson coefficient a_i ($i = 1, 2$). The coefficient a_i varies from process to process but only less than about 1% [1,13,18,21]. It is, therefore, a good approximation to take $a_1 = 1.05$ and $a_2 = 0.25$ for all processes.

In QCD factorization, in the heavy quark limit and to leading order α_s, the current-current amplitude can be factorized into a product of two single quark currents, if weak annihilation contributions are ignored. We neglect here the so-called W exchange and annihilation diagrams; since in the limit $M_W \to \infty$, they are connected by Fiertz transformation and are doubly suppressed by the kinematic factor of the order (M_X^2/M_B^2) [6]. We also discard the color octet currents which emerge after the Fiertz transformation of color-singlet operators. Clearly these currents violate factorization since they can not provide transitions to the vacuum states.

The matrix element of the weak current J_μ between meson states has the covariant decomposition

$$\langle X \mid A_\mu \mid B\rangle = f(q^2)\epsilon^*_\mu + a_+(q^2)(\epsilon^*.P_B)(P_B+P_X)_\mu + a_-(q^2)(\epsilon^*.P_B)(P_B-P_X)_\mu, \tag{3}$$

$$\langle X \mid V_\mu \mid B\rangle = ig(q^2) \in_{\mu\nu\rho\sigma} \epsilon^{*\nu}(P_B+P_X)^\rho(P_B-P_X)^\sigma, \tag{4}$$

where ϵ^* is the polarization vector for the meson X. With 4-momenta $q \equiv (E, 0, 0, |\vec{q}|)$ and mass M_X, the polarization vector is taken in the form

$$\epsilon^\mu_\pm \equiv \frac{1}{\sqrt{2}}(0, \mp 1, -i, 0), \qquad \epsilon^\mu_L \equiv \frac{1}{M_X}(|\vec{q}|, 0, 0, E). \tag{5}$$

The matrix element of the current J^μ between the vacuum and final vector meson state in the covariant form is parametrized by the meson decay constant f_Y as

$$\langle Y|J^\mu|0\rangle = \epsilon^*_Y f_Y M_Y. \tag{6}$$

In the factorization approximation there are three classes of possible diagrams for B meson nonleptonic decays as shown in Fig. 1 which can contribute to the decay amplitude. Figure 1(a) represents "class I" transitions, such as $B^0 \to X^-Y^+$, where only the term with a_1 in Eq. (1) contributes, and both the final state mesons are produced by charged currents. Figure 1(b) represents "class II" transitions such as $B^0 \to X^0Y^0$, where only the term with a_2 in Eq. (1) contributes, and both the final state mesons are produced by neutral currents. Fig. 1(c) represents "class III" transitions such as $B^+ \to X^0Y^+$, where both the terms can contribute coherently.

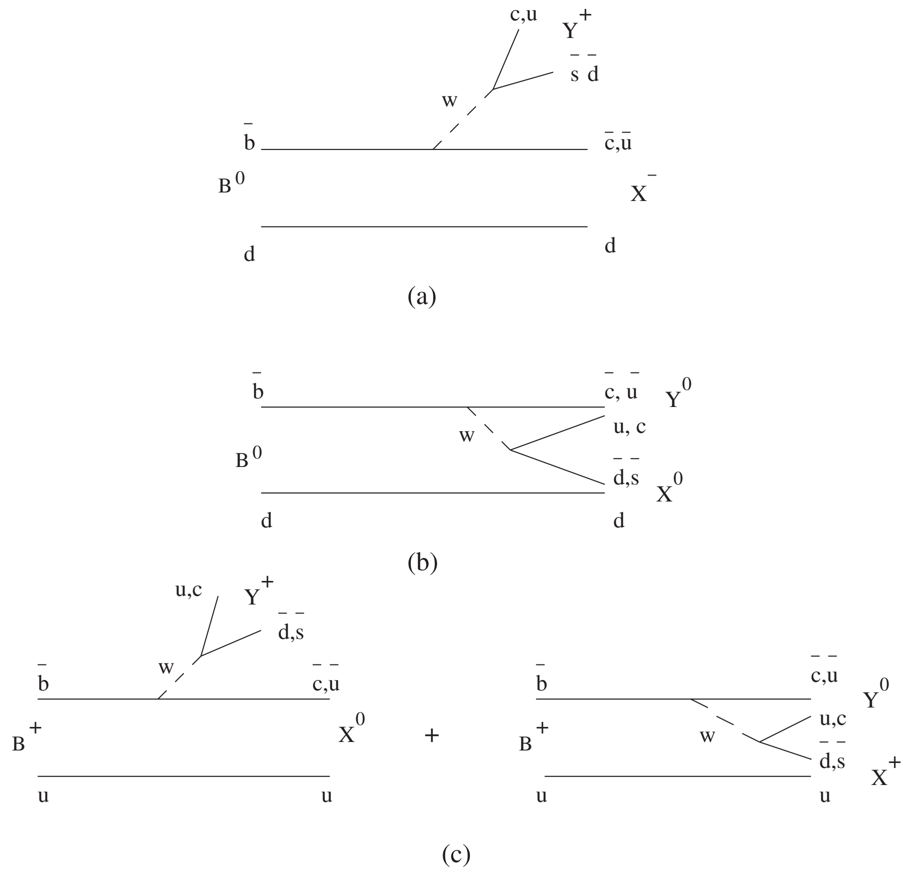

FIG. 1. Quark level diagrams for B meson nonleptonic decays.

For the color favored general-type tree decay $B(\bar{b}q) \to X^-(q\bar{q}')Y^+(q_1\bar{q}_2)$ pertaining to class I transition, the decay rate can be written as

$$\Gamma = \frac{G_F^2}{16\pi} a_1^2 |V_{q'b} V_{q_1 q_2}|^2 \frac{|\vec{q}|}{M_B^2} |\mathcal{A}|^2, \tag{7}$$

where $\vec{q}$ is the recoil 3-momenta in the rest frame of B, and M_B is the B meson mass. $|\mathcal{A}|^2$ is the sum of the squares of the polarization amplitudes $\mathcal{A}_j \equiv \langle Y|J^\mu|0\rangle\langle X|J_\mu|B\rangle$ such that

$$|\mathcal{A}|^2 = \sum_j |\mathcal{A}_j|^2. \tag{8}$$

Here we use the notation $j = +-$, $-+$ or ll, where the first and second label denote the helicity of the X and Y meson, respectively.

The polarized amplitudes $\mathcal{A}_j$ are related to the weak form factors f, g and a_+, and the decay constant f_Y (3)–(6). The resulting relationships for positive, negative, and longitudinal polarization, respectively, of the daughter meson X are obtained in the straightforward manner as

$$\begin{aligned} \mathcal{A}_{+-} &= -f_Y M_Y (f + 2g|\vec{q}|M_B) \\ \mathcal{A}_{-+} &= -f_Y M_Y (f - 2g|\vec{q}|M_B) \\ \mathcal{A}_{ll} &= \frac{f_Y}{M_X}\bigg[f\bigg\{ |\vec{q}|^2 + \frac{1}{4M_B^2}(M_B^2 + M_X^2 - M_Y^2) \\ &\quad \times (M_B^2 + M_Y^2 - M_X^2)\bigg\} + 2a_+|\vec{q}|^2 M_B^2 \bigg]. \end{aligned} \tag{9}$$

Here,

$$|\vec{q}| = \bigg[\bigg(\frac{M_B^2 + M_X^2 - M_Y^2}{2M_B}\bigg)^2 - M_X^2\bigg]^{1/2}.$$

For predicting the decay rate $\Gamma(B \to VV)$, one needs to calculate the relevant weak form factors in a suitable bound state model. Before calculating the form factors in the RIQM, we describe the brief outline of the model framework in the following section.

III. MODEL FRAMEWORK

The model framework based on the relativistic independent quark model has been described earlier to analyze the decays of hadrons in the light as well as heavy flavor sector in their annihilation mode [23–25]. However, for the sake of completeness, here we provide a brief outline of the same. In this model, the decaying meson such as $B^0(\bar{b}d)$ is represented by a suitably constructed definite momentum and spin state $|B(\vec{p}, S_B)\rangle$ in the form of a momentum wave packet reflecting the momentum and spin distribution of its constituent antiquark "$\bar{b}$" and quark "d" as

$$|B(\vec{p}, S_B)\rangle = \frac{\sqrt{3}}{\sqrt{N(\vec{p})}} \sum_{\lambda_b, \lambda_d} \zeta^B_{b,d}(\lambda_b, \lambda_d) \int d^3\vec{p}_b d^3\vec{p}_d \times \delta^{(3)}(\vec{p}_b + \vec{p}_d - \vec{p}) \mathcal{G}_B(\vec{p}_b, \vec{p}_d) \times \hat{b}^\dagger_d(\vec{p}_d, \lambda_d) \hat{\tilde{b}}^\dagger_b(\vec{p}_b, \lambda_b) |0\rangle, \tag{10}$$

where $\hat{b}^\dagger_d(\vec{p}_d, \lambda_d)$ and $\hat{\tilde{b}}^\dagger_b(\vec{p}_b, \lambda_b)$ are the quark and antiquark creation operators, respectively. $\zeta^B_{b,d}(\lambda_b, \lambda_d)$ stands for the appropriate SU(6)-spin flavor coefficient for the meson $B(\bar{b}d)$. $N(\vec{p})$ is the meson-state normalization factor which is realized from $\langle B(\vec{p}) | B(\vec{p}')\rangle = \delta^{(3)}(\vec{p} - \vec{p}')$ in the integral form as

$$N(\vec{p}) = \int d^3\vec{p}_b |\mathcal{G}_B(\vec{p}_b, \vec{p} - \vec{p}_b)|^2. \tag{11}$$

Finally, $\mathcal{G}_B(\vec{p}_b, \vec{p}_d)$ represents the effective momentum distribution function for the quark-antiquark pair inside the meson bound state which is taken in the form

$$\mathcal{G}_B(\vec{p}_b, \vec{p}_d) = [G_d(\vec{p}_d)\tilde{G}_b(\vec{p}_b)]^{1/2}. \tag{12}$$

Here $G_d(\vec{p}_d)$ and $\tilde{G}_b(\vec{p}_b)$ are the momentum probability amplitude of the bound quark (d) with momentum $\vec{p}_d$ and antiquark $\bar{b}$ with momentum $\vec{p}_b$, respectively. The bound quark and antiquark ($d\bar{b}$) inside the meson core are in fact in definite energy states with no definite momenta. However, it is possible to extract the momentum probability amplitude of the bound quark and antiquark inside the meson core from the respective quark-antiquark orbitals derivable in the relativistic independent quark model. In this model, the meson is pictured as a color-singlet assembly of a quark-antiquark ($d\bar{b}$) independently confined by an effective and average flavor independent potential of the form [23–25] $U(r) = \frac{1}{2}(1 + \gamma^0)(ar^2 + V_0)$. It is believed that the zeroth order quark dynamics generated by the phenomenological confining potential $U(r)$ can provide an adequate tree level description of the decay processes: $B \to VV$. With the potential $U(r)$ built into the zeroth order quark Lagrangian density, the ensuing Dirac equation admits static solutions of the positive and negative energy in zeroth order, which for the ground state meson can be obtained in the form

$$\phi^{(+)}_q(\vec{r}, \lambda_q) = \frac{1}{\sqrt{4\pi}} \begin{pmatrix} \frac{ig_q(r)}{r} \\ \frac{\vec{\sigma}.\hat{r} f_q(r)}{r} \end{pmatrix} \chi(\lambda_q)$$
$$\phi^{(-)}_q(\vec{r}, \lambda_q) = \frac{1}{\sqrt{4\pi}} \begin{pmatrix} \frac{i(\vec{\sigma}.\hat{r}) f_q(r)}{r} \\ \frac{g_q(r)}{r} \end{pmatrix} \tilde{\chi}(\lambda_q), \tag{13}$$

where the spinors are

$$\chi(\uparrow) = \begin{pmatrix} 1 \\ 0 \end{pmatrix} = i\tilde{\chi}(\downarrow) \quad \text{and} \quad \chi(\downarrow) = \begin{pmatrix} 0 \\ 1 \end{pmatrix} = -i\tilde{\chi}(\uparrow).$$

The reduced radial parts as the upper and lower components of the quark orbitals in Eq. (6) can be realized in this potential model as

$$g_q(r) = \mathcal{N}_q \left(\frac{r}{r_{0q}}\right) \exp\left(-\frac{r^2}{2r_{0q}^2}\right)$$
$$f_q(r) = -\frac{\mathcal{N}_q}{\omega_q r_{0q}} \left(\frac{r}{r_{0q}}\right)^2 \exp\left(-\frac{r^2}{2r_{0q}^2}\right), \tag{14}$$

where the quark binding energy E_q in the meson ground state is derivable from the bound state condition $(E_q + m_q)(E_q - m_q - V_0)^2 = 9a$. With $E'_q = (E_q - \frac{V_0}{2})$, $m'_q = (m_q + \frac{V_0}{2})$, $\omega_q = (E_q + m_q)$, and $r_{0q} = (a\omega_q)^{-1/4}$, the normalization factor $\mathcal{N}_q$ appearing in Eq. (7) is obtained in the form

$$\mathcal{N}_q^2 = \frac{8\omega_q}{\sqrt{\pi} r_{0q}} \frac{1}{(3E'_q + m'_q)}. \tag{15}$$

Then, by taking suitable momentum space projections of the bound quark-antiquark orbitals in Eqs. (13) and (14), it is straightforward to obtain the momentum probability amplitudes $G_d(\vec{p}_d)$ and $\tilde{G}_b(\vec{p}_b)$ in the form

$$G_d(\vec{p}_d) = \frac{i\pi\mathcal{N}_d}{2\alpha_d\omega_d} \left[\frac{\epsilon_d(\vec{p}_d)}{E_d(\vec{p}_d)}\right]^{1/2} [E_d(\vec{p}_d) + E_d] \exp\left(-\frac{\vec{p}_d^2}{4\alpha_d}\right)$$
$$\tilde{G}_b(\vec{p}_b) = \frac{-i\pi\mathcal{N}_b}{2\alpha_b\omega_b} \left[\frac{\epsilon_b(\vec{p}_b)}{E_b(\vec{p}_b)}\right]^{1/2} [E_b(\vec{p}_b) + E_b] \times \exp\left(-\frac{\vec{p}_b^2}{4\alpha_b}\right). \tag{16}$$

Here $E_q(\vec{p}_q) = \sqrt{\vec{p}_q^2 + m_q^2}$, $\epsilon_q(\vec{p}_q) = (E_q(\vec{p}_q) + m_q) \equiv \epsilon_q$, and $\alpha_q = \frac{1}{(2r_{0q}^2)}$. We may point out here that although 3-momenta conservation at the composite level of the meson has been ensured through $\delta^{(3)}(\vec{p}_b + \vec{p}_d - \vec{p})$ in the expression for the meson state $|B(\vec{p}, S_B)\rangle$ in Eq. (10), the energy conservation $E_B = E_b(\vec{p}_b) + E_d(\vec{p}_d)$ at the meson level is not so explicit here. This is, indeed, a pathological problem common to all such models attempting to explain the hadron decays in terms of constituent level dynamics in zeroth order. However, it is quite reassuring to note here that the effective momentum profile function $\mathcal{G}_B(\vec{p}_b, \vec{p}_d)$, defined through Eqs. (12) and (16) in our model, somehow ensures the energy conservation in an average sense satisfying $E_B = \langle B(\vec{p}, S_B)|[E_b(\vec{p}_b) + E_d(\vec{p}_d)]|B(\vec{p}, S_B)\rangle$ which was shown in our earlier works [26] in the context of radiative leptonic decays of the B_u meson in the present model. However, this point will be illustrated further in the present context for $|B(\vec{p}, S_B)\rangle$ in the appropriate section hereafter.

Now with this phenomenological picture showing detailed dynamics of the constituent quark and antiquark in the meson bound state, we would extract the model expressions for the weak form factors, polarized amplitudes, and the decay width in the following section.

IV. TRANSITION AMPLITUDE AND DECAY WIDTH

As discussed earlier, the transition amplitude for the $B \to VV$ decay mode can be calculated from any of the three diagrams in Fig. 1 depending on the decay process under investigation. Let us consider $B^0 \to D^{*-}D_s^{*+}$ decay which represents the class I transition shown in Fig. 1(a). At the constituent level this process is pictured as the decay of antiquark $\bar{b}$ with 4-momenta p_b inside the meson state $|B(\vec{p})\rangle$ to antiquark $\bar{c}$ with 4-momenta p_c, which along with the spectator quark d with 4-momenta p_d hadronize to the meson state $|D^{*-}(\vec{k})\rangle$. In the process, the externally emitted W boson with 4-momenta q decays to a quark c and an antiquark $\bar{s}$ with 4-momenta p'_c and p'_s, respectively, which subsequently hadronize to the other meson state $|D_s^{*+}(\vec{q})\rangle$. Considering the factorization hypothesis (1) and using the appropriate meson states $|B(\vec{p})\rangle$ and $|D^{*-}(\vec{k})\rangle$, the S-matrix element for the process can be obtained in the form

$$S_{fi} = -i\frac{G_F}{\sqrt{2}}V_{bc}V_{cs}a_1 h'^{\mu}\mathcal{H}'_{\mu}, \tag{17}$$

where

$$h'^{\mu} = \langle D_s^{*+}(\vec{q})|J^{\mu}|0\rangle \tag{18}$$

and

$$\begin{aligned}\mathcal{H}'_{\mu} &= \langle D^{*-}(\vec{k})|J_{\mu}|B(\vec{p})\rangle \\ &= \frac{1}{(2\pi)^2}\frac{1}{\sqrt{N_B(\vec{p})N_{D^{*-}}(\vec{k})}}\int\frac{d\vec{p}_b}{\sqrt{2E_b(\vec{p}_b)2E_c(\vec{p}_b+\vec{k})}} \\ &\quad \times G_B(\vec{p}_b,\vec{p}_d)G_{D^{*-}}(\vec{p}_b+\vec{k},\vec{p}_d) \\ &\quad \times \delta^{(4)}(p_b - p_c - p'_c - p'_s)\langle S_{D^{*-}}|J_{\mu}|S_B\rangle. \end{aligned}\tag{19}$$

Here $E_b(\vec{p}_b) = \sqrt{\vec{p}_b{}^2 + m_b^2}$ and $E_c(\vec{p}_b+\vec{k}) = \sqrt{(\vec{p}_b+\vec{k})^2 + m_c^2}$ stand for the energy of the nonspectator quark of the B and D^{*-} meson, respectively. $\langle S_{D^{*-}}|J_{\mu}|S_B\rangle$, which symbolically represents the spin matrix elements due to vector-axial vector current, is given by

$$\begin{aligned}\langle S_{D^{*-}}|J_{\mu}|S_B\rangle = &\sum_{\lambda_b,\lambda_c,\lambda_d}\zeta^B(\lambda_b,\lambda_d)\zeta^{D^{*-}}(\lambda_c,\lambda_d)\bar{U}_c(\vec{p}_b+\vec{k},\lambda_c) \\ &\times\gamma_{\mu}(1-\gamma^5)U_b(\vec{p}_b,\lambda_b),\end{aligned}\tag{20}$$

where the free particle spinors $U_q(\vec{p}_q,\lambda_q)$ are taken in the form

$$U_q(\vec{p}_q,\lambda_q) = \sqrt{\epsilon_q(\vec{p}_q)}\begin{pmatrix}\chi(\lambda_q) \\ \frac{\vec{\sigma}.\vec{p}_q}{\epsilon(\vec{p}_q)}\chi(\lambda_q)\end{pmatrix} \tag{21}$$

with

$$\chi(\uparrow) = -\tilde{\chi}(\downarrow) = \begin{pmatrix}1\\0\end{pmatrix}, \qquad \chi(\downarrow) = \tilde{\chi}(\uparrow) = \begin{pmatrix}0\\1\end{pmatrix}.$$

It may be noted here that in the present model, the energy conservation at the composite level is expected to be satisfied in an average sense through the momentum distribution function $\mathcal{G}_B(\vec{p}_b,\vec{p}_d)$ and $\mathcal{G}_{D^{*-}}(\vec{p}_c,\vec{p}_d)$. Therefore we may assume $E_B = E_b(\vec{p}_b) + E_d(\vec{p}_d)$ and $E_{D^{*-}} = E_c(\vec{p}_b+\vec{k}) + E_d(\vec{p}_d)$, which together with the 3-momenta conservation $\vec{p} = \vec{p}_b + \vec{p}_d$ and $\vec{k} = (\vec{p}_c + \vec{p}_d)$ ensured by $\delta^3(\vec{p} - \vec{p}_b - \vec{p}_d)$ and $\delta^3(\vec{k} - \vec{p}_c - \vec{p}_d)$ appearing, respectively, in the meson states $|B(\vec{p})\rangle$ and $|D^{*-}(\vec{k})\rangle$, can enable us to write $p = (p_b + p_d)$ and $k = (p_c + p_d)$. With this assumption, we pull out $\delta^{(4)}(p_b - p_c - p'_c - p'_s)$ appearing in S_{fi} (17) from the quark level integral in the form $\delta^{(4)}(p-q-k)$ that ensures the desired 4-momenta conservation in the decay process. Then we can write

$$S_{fi} = (2\pi)^4\delta^{(4)}(p-q-k)[-i\mathcal{M}_{fi}]\prod_f\left(\frac{1}{(2\pi)^{3/2}}\frac{1}{\sqrt{2E_f}}\right). \tag{22}$$

We may further point out that the normalization factors $\frac{1}{\sqrt{(2\pi)^3 2E_B}}$, $\frac{1}{\sqrt{(2\pi)^3 2E_{D^{*-}}}}$ and $\frac{1}{\sqrt{(2\pi)^3 2E_{D_s^{*+}}}}$ for the initial and final meson states do not appear automatically in the kinematic expression (22) for S_{fi}. We, therefore, incorporate these factors by adequately compensating the same in the numerator. The compensating factor $\sqrt{2E_B 2E_{D^{*-}}}$ relevant for the matrix element $\mathcal{H}'_{\mu} = \langle D^{*-}(\vec{k})|J_{\mu}|B(\vec{p})\rangle$ is then pushed inside the integral as $\sqrt{2(E_b(\vec{p}_b) + E_d(\vec{p}_d))}\sqrt{2(E_c(\vec{p}_c) + E_d(\vec{p}_d))}$ under the same assumption of the energy conservation mentioned earlier to be expressed hereafter as $\mathcal{H}_{\mu}$. The factor $\sqrt{2E_{D_s^{*+}}}$ together with $\langle D_s^{*+}(\vec{k})|J^{\mu}|0\rangle$ defines the covariant matrix element which can be parametrized as $(M_{D_s^{*+}}f_{D_s^{*+}}\epsilon^{*\mu}_{D_s^{*+}})$. Thus realizing the meson level S-matrix element for the decay process in the desired form, the corresponding invariant transition amplitude in the rest frame of the B meson is extracted as

$$\mathcal{M}_{fi} = \frac{G_F}{\sqrt{2}}V_{bc}V_{cs}a_1\mathcal{A}. \tag{23}$$

Here $\mathcal{A} = h^{\mu}\mathcal{H}_{\mu}$ represents the polarized amplitude with

$$h^{\mu} \equiv \sqrt{2E_{D_s^{*+}}}h'^{\mu} = M_{D_s^{*+}}f_{D_s^{*+}}\epsilon^{*\mu}_{D_s^{*+}}(\vec{q},\lambda), \tag{24}$$

and the hadronic term $\mathcal{H}_{\mu}$ is obtained in the form

$$\mathcal{H}_{\mu}=\frac{1}{(2\pi)^{3/2}}\frac{1}{\sqrt{N_B(0)N_{D^{*-}}(\vec{k})}}\int\frac{d\vec{p}_b}{\sqrt{2E_b(\vec{p}_b)2E_c(\vec{p}_b+\vec{k})}}\times G_B(\vec{p}_b,-\vec{p}_b)G_{D^{*-}}(\vec{p}_b+\vec{k},-\vec{p}_b)\times\sqrt{2(E_b(\vec{p}_b)+E_d(-\vec{p}_b))2(E_c(\vec{p}_b+\vec{k})+E_d(-\vec{p}_b))}\times\langle S_{D^{*-}}|J_{\mu}|S_B\rangle. \quad (25)$$

Now applying the usual spin algebra to calculate the spin matrix elements $\langle S_{D^{*-}}|(V_{\mu}-A_{\mu})|S_B\rangle$, it is easy to check that the matrix element due to the vector current provides nonvanishing spacelike contribution. However, the contribution of the matrix element due to the axial vector current is both spacelike and timelike. The nonvanishing contributions obtained separately due to the vector and axial vector currents are found in the following form:

$$\mathcal{H}_i=\langle D^{*-}(\vec{k})\mid V_i\mid B^0(0)\rangle = i\int d\vec{p}_b\mathcal{Q}(\vec{p}_b)(E_b(\vec{p}_b)+m_b)(\vec{\epsilon}^{*}(\vec{k},\lambda)\times\vec{k})_i, \quad (26)$$

$$\mathcal{H}_0^5=\langle D^{*-}(\vec{k})\mid A_0\mid B^0(0)\rangle = -\int d\vec{p}_b\mathcal{Q}(\vec{p}_b)(\vec{\epsilon}^{*}(\vec{k},\lambda)\cdot\vec{k}), \quad (27)$$

$$\mathcal{H}_i^5=\langle D^{*-}(\vec{k})\mid A_i\mid B^0(0)\rangle = -\int d\vec{p}_b\mathcal{R}(\vec{p}_b)\epsilon_i^{*}(\vec{k},\lambda), \quad (28)$$

when

$$\mathcal{Q}(\vec{p}_b)=\sqrt{\frac{[E_b(\vec{p}_b)+E_d(-\vec{p}_b)][(E_c(\vec{p}_b+\vec{k})+E_d(-\vec{p}_b)]}{N_{B^0}(0)N_{D^{*-}}(\vec{k})}}\times\frac{\mathcal{G}_{B^0}(\vec{p}_b,-\vec{p}_b)\mathcal{G}_{D^{*-}}(\vec{p}_b+\vec{k},-\vec{p}_b)}{\sqrt{E_b(\vec{p}_b)E_c(\vec{p}_b+\vec{k})(E_b(\vec{p}_b)+m_b)(E_c(\vec{p}_b+\vec{k})+m_c)}} \quad (29)$$

and

$$\mathcal{R}(\vec{p}_b)=\mathcal{Q}(\vec{p}_b)(E_b(\vec{p}_b)+m_b)(E_c(\vec{p}_b+\vec{k})+m_c)\times\left[1-\frac{\vec{p}_b^{\,2}}{3(E_b(\vec{p}_b)+m_b)(E_c(\vec{p}_b+\vec{k})+m_c)}\right]. \quad (30)$$

These model expressions are compared with the corresponding expressions from Eqs. (3) and (4), which yield model expressions for the relevant weak form factors in the form

$$g(q^2)=-\frac{1}{2M_B}\int d\vec{p}_b\mathcal{Q}(\vec{p}_b)(E_b(\vec{p}_b)+m_b), \quad (31)$$

$$f(q^2)=-\int d\vec{p}_b\mathcal{R}(\vec{p}_b), \quad (32)$$

and

$$a_+(q^2)=a_-(q^2) = -\frac{1}{2M_B^2}\left[(E_{D^{*-}})\int d\vec{p}_b\mathcal{Q}(\vec{p}_b)-\int d\vec{p}_b\mathcal{R}(\vec{p}_b)\right]. \quad (33)$$

We then find the polarized amplitude squared $|\mathcal{A}_j|^2$ from Eq. (9) and carry out the polarization sum $\sum_j|\mathcal{A}_j|^2$. Finally, we integrate over the final particles (D^{*-},D_s^{*+}) momenta to obtain the expression of the decay width $\Gamma(B\to D^{*-}D_s^{*+})$ in the B-rest frame from its generic expression,

$$\Gamma(B^0\to D^{*-}D_s^{*+})=\frac{1}{(2\pi)^2}\int\frac{d\vec{k}d\vec{q}}{2M_B2E_{D^{*-}}2E_{D_s^{*+}}}\times\delta^{(4)}(p-k-q)\bar{\sum}|\mathcal{M}_{fi}|^2, \quad (34)$$

in the forms (7)–(9). The magnitude of 3-momenta transfer $\vec{q}$ appearing in the final expression for helicity amplitude squared in $\Gamma(B^0\to D^{*-}D_s^{*+})$ is fixed by the argument factorization of the energy delta function as

$$|\vec{q}|=\left[\left(\frac{M_B^2+M_{D^{*-}}^2-M_{D_s^{*+}}^2}{2M_B}\right)^2-M_{D^{*-}}^2\right]^{1/2}. \quad (35)$$

The class II transitions [Fig. 1(b)] such as $B^0\to D^{*0}K^{*0}$, are described at the constituent level as the decay of antiquark $\bar{b}$ to another antiquark with the internal emission of the W boson, which subsequently decays to a pair of quark-antiquark. Three constituent particles so emitted in the process along with the spectator quark d of the parent meson finally hadronize to two vector mesons by two neutral currents. The transition amplitudes of these decays are derived from the factorized amplitudes associated with the effective Wilson coefficient a_2 instead of a_1. The class III transitions of the type $B^+\to\bar{D}^{*0}\rho^+$, however, involve the antiquark $\bar{b}$ decay with both the external and internal W emission as shown in Fig. 1(c). In these decays the contribution from both the diagrams, in principle, add up at the amplitude level to give the transition amplitude. However, for some specific channels in the class III transition like $B^+\to\bar{D}^{*0}D_s^{*+}$, the factorized amplitudes associated with a_1 only contribute as the diagram corresponding to the a_2 term is not kinematically possible. The decay width expression for all other $B\to VV$ channels belonging to class I, class II, and class III transitions can be obtained from Eqs. (7)–(9) through (29)–(33) by replacement with appropriate flavor degrees of freedom, quark masses, meson masses, meson decay constants, and the effective Wilson coefficient a_i.

V. RESULT AND DISCUSSION

For numerical calculations, we take the potential parameters (a, V_0) and the quark masses along with the corresponding quark binding energies as in Refs. [23–26],

$$\begin{aligned}(a; V_0) &\equiv (0.017\,166\ \mathrm{GeV}^3; -0.1375\ \mathrm{GeV})\\ (m_u = m_d; m_s) &\equiv (0.07\,875\ \mathrm{GeV}; 0.31\,575\ \mathrm{GeV})\\ (m_c; m_b) &\equiv (1.49\,276\ \mathrm{GeV}; 4.77\,659\ \mathrm{GeV})\\ (E_u = E_d; E_s) &\equiv (0.47\,125\ \mathrm{GeV}; 0.591\ \mathrm{GeV})\\ (E_c; E_b) &\equiv (1.57\,951\ \mathrm{GeV}; 4.76\,633\ \mathrm{GeV}).\end{aligned} \tag{36}$$

We take into account the central values of the CKM parameters, the half life of B^0 and B^+, and the observed meson masses from the Particle Data Group [27] as

$$\begin{aligned}(V_{cb}; V_{cs}; V_{cd}) &\equiv (0.0412; 1.04; 0.23)\\ (V_{ub}; V_{us}; V_{ud}) &\equiv (0.00\,393; 0.2255; 0.97\,418)\\ (\tau_{\bar{B}^0}; \tau_{B^+}) &\equiv (1.530\ \mathrm{ps}, 1.638\ \mathrm{ps})\\ (M_{B^0}; M_{B^+}) &\equiv (5.2795\ \mathrm{GeV}; 5.2791\ \mathrm{GeV}).\end{aligned} \tag{37}$$

In the absence of reliable experimental data for the meson decay constants, we take their values equal to the corresponding pseudoscalar meson decay constants obtained earlier in the present model [28] in GeV units as

$$\begin{aligned}&f_\rho = 0.22; \qquad f_K \equiv f_{K^*} = 0.157;\\ &f_D \equiv f_{D^*} = 0.161; \qquad f_{D_s} \equiv f_{D_s^*} = 0.205.\end{aligned} \tag{38}$$

As discussed earlier, we take the effective Wilson coefficients a_1 and a_2 as

$$(a_1, a_2) \equiv (1.05, 0.25). \tag{39}$$

At the outset we must point out that we have assumed energy conservation constraint $E_b(\vec{p}_b) + E_{d,u}(\vec{p}_{d,u}) = E_B$, which together with the 3-momenta conservation through $\delta^{(3)}(\vec{p} - \vec{p}_b - \vec{p}_d)$ in the meson state, $|B(\vec{p}, S_B)\rangle$ is thought to ensure the required 4-momenta conservation. However, imposition of this energy conservation constraint $E_b(\vec{p}_b) + E_{d,u}(-\vec{p}_b) = M_B$ corresponding to the rest frame of the decaying B meson may present spurious kinematic singularities. This can be dealt with as in Ref. [29] by retaining the definite spectator quark mass $m_{d,u}$ while assigning a running mass $m_b(\vec{p}_b)$ to the b quark in the form

$$m_b^2(|\vec{p}_b|) = M_B^2 + m_{u,d}^2 - 2M_B\sqrt{|\vec{p}_b|^2 + m_{u,d}^2} \tag{40}$$

as an outcome of $M_B = E_b(\vec{p}_b) + E_{d,u}(-\vec{p}_b)$. This would impose an upper bound on the momentum $|\vec{p}_b| < \frac{M_B^2 - m_{u,d}^2}{2M_B} = |\vec{p}_b|_{\max}$ in order to retain $m_b^2(|\vec{p}_b|)$ positive definite.

The upper limit $|\vec{p}_b|_{\max}$ of the quark momentum would have no other bearing to seriously affect the calculation, which is apparent from the shape of the radial quark momentum distribution amplitude $|\vec{p}_b|\mathcal{G}_B(\vec{p}_b, -\vec{p}_b)$ shown in Fig. 2. The radial quark momentum distribution in the present model is very similar to that obtained in the QCD relativistic model [29,30]. From the expectation value $\langle B(0)|\vec{p}_b^2|B(0)\rangle = \langle \vec{p}_b^2\rangle$, we find the rms value of the quark momentum in the state $|B(0)\rangle$ as $\sqrt{\langle \vec{p}_b^2\rangle} = 0.51\ \mathrm{GeV} \ll |\vec{p}_b|_{\max}$. The expectation values of the quark and antiquark binding energies are obtained as $\langle E_b(\vec{p}_b)\rangle = 4.799$ GeV and $\langle E_{d,u}(-\vec{p}_b)\rangle = 0.480$ GeV, which are very close to the respective model solutions for the quark binding energies E_b and $E_{d,u}$ in Eq. (36). We also find that $\langle B(0)|[E_b(\vec{p}_b) + E_{u,d}(-\vec{p}_b)]|B(0)\rangle = 5.279\ \mathrm{GeV} = M_B$. These results vindicate our ansatz that energy conservation is somehow ensured by the quark momentum distribution in the meson state in an average sense.

With the values of model parameters and other relevant physical quantities (36)–(39), we first evaluate the form factors f, g, and a_+ from Eqs. (29)–(33) and then predict the BRs for $B \to VV$ decays as shown in Table I. Our predictions for class I transitions are found in agreement with the experiment, and those for class II and class III are mostly within the experimental limits. A scrutiny of our results shows that the contributions from a_2 terms in those class III transitions involving both the internal and external W emission are small compared to those obtained in other models [12,13]. This may be due to different q^2 dependence of $B \to \rho(k^*)$ transition form factors (Fig. 3) in the present model.

The predicted form factors along with their q^2 behavior and the branching ratios for $B \to VV$ decays have been shown to vary in the same order of magnitude in various model dependent studies. This is not surprising, since uncertainties in the predictions may come mainly from two counts. (i) Since the decay amplitudes are proportional to the meson decay constants, the predictions would change from one model study to other using different

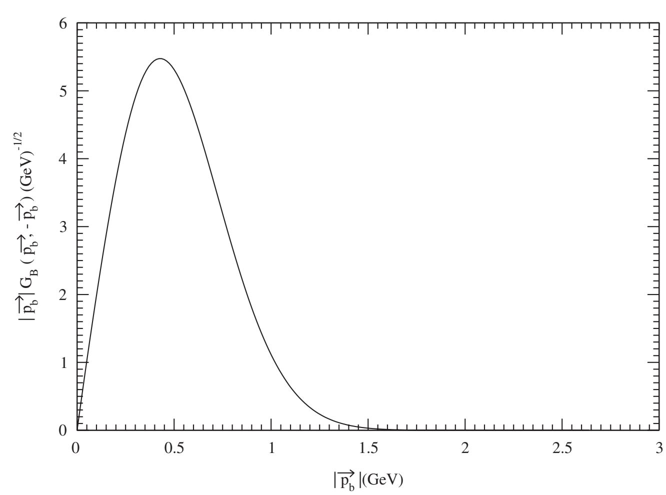

FIG. 2. Radial quark momentum distribution amplitude $|\vec{p}_b|\mathcal{G}_B(\vec{p}_b, -\vec{p}_b)$ versus $|\vec{p}_b|$.

TABLE I. Predicted branching ratios for $B \to VV$ nonleptonic decays (in percent) in comparison with the experimental data.

Decays	Our result	Our result	Experiment [27]
$B^0 \to D^{*-} D_s^{*+}$	$1.74a_1^2$	1.92	(1.79 ± 0.14)
$B^0 \to D^{*+} D^{*-}$	$0.0512a_1^2$	0.0565	(0.082 ± 0.009)
$B^0 \to D_s^{*+} \rho^-$	$0.0035a_1^2$	0.0039	<0.06
$B^0 \to D^{*-} \rho^+$	$1.27a_1^2$	1.40	(0.68 ± 0.09)
$B^0 \to \bar{D}^{*0} \rho^0$	$0.1888a_2^2$	0.0118	<0.051
$B^0 \to \bar{D}^{*0} \omega$	$0.1856a_2^2$	0.0116	(0.027 ± 0.008)
$B^0 \to D^{*0} K^{*0}$	$0.0048a_2^2$	0.0003	<0.004
$B^0 \to \bar{D}^{*0} K^{*0}$	$0.025a_2^2$	0.0016	<0.0069
$B^+ \to \bar{D}^{*0} D_s^{*+}$	$1.86a_1^2$	2.06	(1.75 ± 0.23)
$B^+ \to \bar{D}^{*0} D^{*+}$	$0.055a_1^2$	0.0606	(0.081 ± 1.7)
$B^+ \to D_s^{*+} \rho^0$	$0.00378a_1^2$	0.00418	<0.04
$B^+ \to D_s^{*+} \omega$	$0.00374a_1^2$	0.00412	<0.06
$B^+ \to \bar{D}^{*0} K^{*+}$	$0.04(a_1 + 0.842a_2)^2$	0.0603	(0.081 ± 0.014)
$B^+ \to \bar{D}^{*0} \rho^+$	$1.4(a_1 + 0.385a_2)^2$	1.79	(0.98 ± 0.17)

decay constants. (ii) The form factors and their q^2 behavior depend typically on the model assumptions. For example, some models assume universal q^2 dependence of the relevant form factors [12], while others do not. We would like to present here the q^2 dependence of the form factors of a representative $B \to D^*$ transition. The form factors f, g, and a_+ in their dimensionless forms

$$\begin{aligned} V(q^2) &= (M_B + M_{D^*})g(q^2) \\ A_1(q^2) &= (M_B + M_{D^*})^{-1} f(q^2) \\ A_2(q^2) &= -(M_B + M_{D^*})a_+(q^2) \\ A_0(q^2) &= \frac{1}{2M_{D^*}}\bigg[(M_B + M_{D^*})A_1 \\ &\quad - \frac{(M_B^2 - M_{D^*}^2 + M_{D_s^*}^2)A_2}{(M_B + M_{D^*})}\bigg] \end{aligned} \tag{41}$$

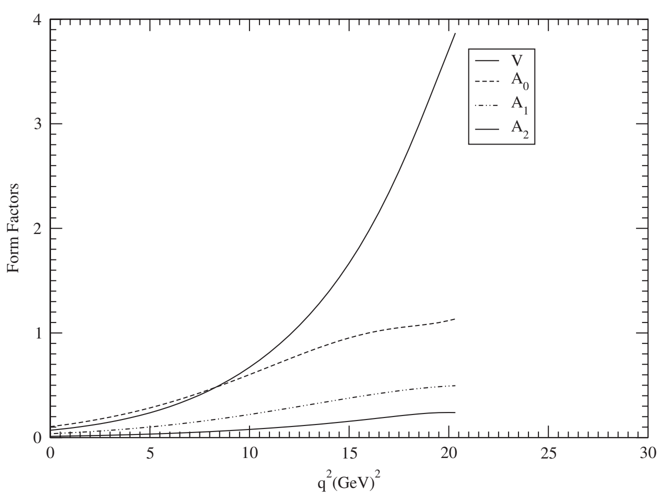

FIG. 3. The q^2 dependence of form factors of $B \to \rho$ transitions.

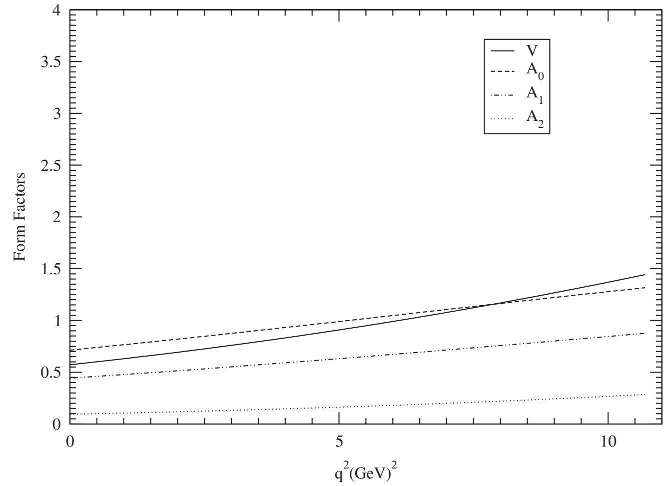

FIG. 4. The q^2 dependence of form factors of $B \to D^*$ transitions.

and their q^2 dependence in the present model are shown in Fig. 4, which are found comparable to those obtained in other models [12,13] for all form factors except for $V(q^2)$. The values of these form factors at $q^2 \to 0$ and $q^2 \to q^2_{\rm max}$ for $B \to D^*$ transition in the present approach are given in Table II.

Our results for BRs are found slightly lower in comparison to those in other models [12–16,21]. However, present experimental data for most of these decay modes can not distinguish which model is more preferred. More precise data are necessary to help constrain the q^2 behavior of the transition form factors and test the validity of the factorization approximation in the study of $B \to VV$ decays in various bound state models. As expected, we also find that the BRs for the neutral B decays are smaller than those for the charged B decays, which may be due to the spectator interaction effects of the d and u quark, respectively.

Our prediction for longitudinal polarization fractions: $R_L = \frac{|A_{ll}|^2}{|A_{+-}|^2 + |A_{-+}|^2 + |A_{ll}|^2}$ for different decay modes are presented in Table III. The predicted R_L's for $B^0 \to D^{*-}(D_s^{*+}, D^{*-}, \rho^+)$ and $B^+ \to \bar{D}^*(\rho^+, K^{*+})$ decays are obtained in agreement with the available experimental data. We find that all the $B \to VV$ decays studied here are found in a more dominant longitudinal mode compared to other model predictions [12–16,21].

TABLE II. Values of form factors at $q^2 = 0$ and $q^2 = q^2_{\rm max}$ for $B \to D^*$ transition.

Form factor	$q^2 = 0$	$q^2 = q^2_{\rm max}$
$V(q^2)$	0.57	1.44
$A_1(q^2)$	0.44	0.87
$A_2(q^2)$	0.10	0.28
$A_0(q^2)$	0.71	1.32

TABLE III. Predicted longitudinal polarization fraction R_L for $B \to VV$ nonleptonic decays in comparison with the experiment.

Decay mode	CQM	LF	HQS	Our result	Experiment [27]
$B^0 \to D^{*-} D_s^{*+}$	0.523	0.512	0.55	0.647	(0.52 ± 0.05)
$B^0 \to D^{*+} D^{*-}$	0.547	0.535	0.538	0.675	$0.57 \pm 0.08 \pm 0.02$
$B^0 \to D_s^{*+} \rho^-$	⋯	⋯	⋯	0.921	⋯
$B^0 \to D^{*-} \rho^+$	⋯	⋯	⋯	0.945	$(0.885 \pm 0.016 \pm 0.012)$
$B^0 \to \bar{D}^{*0} \rho^0$	⋯	⋯	⋯	0.931	⋯
$B^0 \to \bar{D}^{*0} \omega$	⋯	⋯	⋯	0.929	⋯
$B^0 \to D^{*0} K^{*0}$	⋯	⋯	⋯	0.915	⋯
$B^0 \to \bar{D}^{*0} K^{*0}$	⋯	⋯	⋯	0.915	⋯
$B^+ \to \bar{D}^{*0} D_s^{*+}$	0.524	0.512	0.512	0.647	⋯
$B^+ \to \bar{D}^{*0} D^{*+}$	0.547	0.535	0.538	0.676	⋯
$B^+ \to D_s^{*+} \rho^0$	⋯	⋯	⋯	0.921	⋯
$B^+ \to D_s^{*+} \omega$	⋯	⋯	⋯	0.919	⋯
$B^+ \to \bar{D}^{*0} K^{*+}$	⋯	⋯	⋯	0.924	$(0.86 \pm 0.06 \pm 0.03)$
$B^+ \to \bar{D}^{*0} \rho^+$	⋯	⋯	⋯	0.943	$(0.892 \pm 0.018 \pm 0.016)$

Another area that arouses a great deal of interest is the study of the CP violation in $B \to D^* D^*$, $D^* D_s^*$ decays and the test of new physics. This aspect can be assessed in evaluating the CP-odd fraction $R_\perp$ which is related to the helicity amplitudes in the form

$$R_\perp = \frac{|A_{+-} - A_{-+}|^2}{2(|A_{+-}|^2 + |A_{-+}|^2 + |A_{ll}|^2)}.$$

For color-allowed $B \to D^* D^*$ and $D^* D_s^*$ decays, the effects arising out of the short distance nonspectator contributions is shown to be small [31]. However, the long distance (LD) nonfactorizable contributions governed by the rescattering effects or final state interactions may not be negligible in these cases. If there exists a significant LD effect, one expects a large value of the CP-odd fraction ($R_\perp$) to appear in these decays. The predicted $R_\perp$'s, in the present scheme, for different $B \to VV$ decays are shown in Table IV. Our results for two charmful final states, i.e., $D^* D^*$ and $D^* D_s^*$ are broadly in agreement with the experiment remaining within the experimental limit: $0.125 \pm 0.043(\text{stat}) \pm 0.023(\text{syst})$ [10].

TABLE IV. Predicted CP-odd fraction $R_\perp$ for $B \to VV$ nonleptonic decays in the RIQM model.

Decay mode	CQM	LF	HQS	Our result
$B^0 \to D^{*-} D_s^{*+}$	0.069	0.077	0.055	0.063
$B^0 \to D^{*+} D^{*-}$	0.069	0.077	0.055	0.060
$B^0 \to D_s^{*+} \rho^-$	⋯	⋯	⋯	0.052
$B^0 \to D^{*-} \rho^+$	⋯	⋯	⋯	0.013
$B^0 \to \bar{D}^{*0} \rho^0$	⋯	⋯	⋯	0.046
$B^0 \to \bar{D}^{*0} \omega$	⋯	⋯	⋯	0.047
$B^0 \to D^{*0} K^{*0}$	⋯	⋯	⋯	0.048
$B^0 \to \bar{D}^{*0} K^{*0}$	⋯	⋯	⋯	0.048
$B^+ \to \bar{D}^{*0} D_s^{*+}$	0.070	0.078	0.055	0.063
$B^+ \to \bar{D}^{*0} D^{*+}$	0.069	0.077	0.055	0.060
$B^+ \to D_s^{*+} \rho^0$	⋯	⋯	⋯	0.052
$B^+ \to D_s^{*+} \omega$	⋯	⋯	⋯	0.053
$B^+ \to \bar{D}^{*0} K^{*+}$	⋯	⋯	⋯	0.030
$B^+ \to \bar{D}^{*0} \rho^+$	⋯	⋯	⋯	0.023

The large values of the predicted $R_\perp$'s for the modes with two charmful final states compared to those obtained in other modes vindicate the assumption that the nonvanishing LD contributions lead to significant CP violation in $B \to D^* D^*$ and $D^* D_s^*$ decays. Our predictions on $R_\perp$'s for all $B \to VV$ decays including $B \to D^* D^*$ and $D^* D_s^*$ are, in fact, found slightly smaller in comparison with other model predictions [12–16,21]. This may be due to large helicity amplitude A_{ll} and a small value of the form factor g obtained in the present model.

VI. SUMMARY AND CONCLUSION

We have calculated the branching ratio, longitudinal polarization fraction, and the CP-odd fraction of $B \to VV$ decays, within factorization approximation, in the RIQM based on the confining potential in the scalar-vector harmonic form. The predicted branching ratios are found in general agreement with the available experimental data and compared to other model predictions. However, the decay modes studied here are found in a rather more dominant longitudinal mode compared to most other model predictions, of course, remaining within the experimental limit. The CP-odd fraction (0.060, 0.063) obtained in $B \to D^* D^*$, $D^* D_s^*$ modes, respectively, in particular, indicate significant CP violation in this sector.

In conclusion, our study shows that factorization works well also in the B meson heavy-heavy decays in the RIQM-model framework. More precise data would provide better justification of the factorization hypothesis and applicability of the RIQM model in this sector.

ACKNOWLEDGMENTS

Sk. N. acknowledges the financial assistance from the University Grants Commission, New Delhi, under X-Plan Minor Research Project scheme to facilitate the work. We are also thankful to the Institute of Physics, Bhubaneswar, Orissa, for providing the necessary library and computational facilities.

[1] M. Wirbel, B. Stech, and M. Bauer, Z. Phys. C **29**, 637 (1985); M. Bauer, B. Stech, and M. Wirbel, Z. Phys. C **34**, 103 (1987); L.-L. Chau, H.-Y. Cheng, W. K. Sze, H. Yao, and B. Tseng, Phys. Rev. D **43**, 2176 (1991); Ling-Lie Chau, Hai-Yang Cheng, W. K. Sze, Herng Yao, and Benjamin Tseng, Phys. Rev. D **58**, 019902 (1998).

[2] A. Ali, G. Kramer, and C. D. Lu, Phys. Rev. D **58**, 094009 (1998); C. D. Lu, Nucl. Phys. B, Proc. Suppl. **74**, 227 (1999).

[3] Y.-H. Chen, H.-Y. Cheng, B. Tseng, and K.-C. Yang, Phys. Rev. D **60**, 094014 (1999); H.-Y. Cheng and K.-C. Yang, Phys. Rev. D **62**, 054029 (2000).

[4] M. Beneke, G. Buchalla, M. Neubert, and C. T. Sachrajda, Phys. Rev. Lett. **83**, 1914 (1999); Nucl. Phys. **B591**, 313 (2000); **B606**, 245 (2001).

[5] Y. Y. Keum, H.-N. Li, and A. I. Sanda, Phys. Lett. B **504**, 6 (2001); Phys. Rev. D **63**, 054008 (2001); C. D. Lu, K. Ukai, and M. Z. Yang, Phys. Rev. D **63**, 074009 (2001); C. D. Lu and M. Z. Yang, Eur. Phys. J. C **23**, 275 (2002).

[6] A. J. Buras, J. M. Gerard, and R. Ruckl, Nucl. Phys. **B268**, 16 (1986).

[7] J. D. Bjorken, in *Proceedings of the International Workshop on Developments in High Energy Physics, Crete, Greece, 1988*, edited by G. Branco and J. Romao [Nucl. Phys. B, Proc. Suppl. 11, 325 (1989)].

[8] M. Neubert, Phys. Rep. **245**, 259 (1994).

[9] M. J. Dugan and B. Grinstein, Phys. Lett. B **255**, 583 (1991); C. Reader and N. Isgur, Phys. Rev. D **47**, 1007 (1993).

[10] K. Vervink, Ph.D. thesis, Ecole Polytechnique Federale de Lausanne, 2008.

[11] B. Aubert *et al.* (BABAR Collaboration), Phys. Rev. D **76**, 111102(R) (2007).

[12] M. Neubert, V. Rieckert, B. Stech, and Q. P. Xu, in *Heavy Flavours*, edited by A. J. Buras and H. Lindner (World Scientific, Singapore, 1992), p. 286.

[13] D. Ebert, R. N. Faustov, and V. O. Galkin, Phys. Rev. D **56**, 312 (1997).

[14] D. Melikhov and B. Stech, Phys. Rev. D **62**, 014006 (2000).

[15] H. Y. Cheng, C. K. Chua, and C. W. Hwang, Phys. Rev. D **69**, 074025 (2004).

[16] M. Neubert and V. Rieckert, Nucl. Phys. **B382**, 97 (1992); C. H. Chen, C.-Q. Geng, and Z.-T. Wei, Eur. Phys. J. C **46**, 367 (2006).

[17] D. Scora and N. Isgur, Phys. Rev. D **52**, 2783 (1995).

[18] Z. Luo and J. L. Rosner, Phys. Rev. D **64**, 094001 (2001).

[19] C.-H. Chen, C.-Q. Geng, and Z. T. Wei, Eur. Phys. J. C **46**, 367 (2006).

[20] A. Datta and P. J. O'Donnell, Phys. Lett. B **572**, 164 (2003).

[21] C. E. Thomas, Phys. Rev. D **73**, 054016 (2006).

[22] H.-Y. Cheng, Phys. Rev. D **68**, 094005 (2003).

[23] N. Barik, S. Kar, and P. C. Dash, Phys. Rev. D **63**, 114002 (2001).

[24] N. Barik, P. C. Dash, and A. R. Panda, Phys. Rev. D **46**, 3856 (1992); N. Barik and P. C. Dash, *ibid.* **49**, 299 (1994); Mod. Phys. Lett. A **10**, 103 (1995); N. Barik, S. Kar, and P. C. Dash, Phys. Rev. D **57**, 405 (1998); N. Barik, Sk. Naimuddin, S. Kar, and P. C. Dash, Phys. Rev. D **63**, 014024 (2000); N. Barik, P. C. Dash, and A. R. Panda, Phys. Rev. D **47**, 1001 (1993); N. Barik and P. C. Dash, Phys. Rev. D **53**, 1366 (1996); N. Barik, S. K. Tripathy, S. Kar, and P. C. Dash, *ibid.* **56**, 4238 (1997); N. Barik, S. Kar, and P. C. Dash, Phys. Rev. D **63**, 114002 (2001).

[25] N. Barik, Sk. Naimuddin, P. C. Dash, and Susmita Kar, Phys. Rev. D **77**, 014038 (2008).

[26] N. Barik, P. C. Dash, and A. R. Panda, Phys. Rev. D **46**, 3856 (1992); **47**, 1001 (1993).

[27] C. Amsler *et al.* (Particle Data Group), Phys. Lett. B **667**, 1 (2008).

[28] N. Barik, P. C. Dash, and A. R. Panda, Phys. Rev. D **47**, 1001 (1993); N. Barik and P. C. Dash, *ibid.* **47**, 2788 (1993).

[29] P. Colangelo, F. De Fazio, and G. Nardulli, Phys. Lett. B **386**, 328 (1996).

[30] G. Altarelli, N. Cabibbo, G. Corbo, L. Maiani, and G. Martinelli, Nucl. Phys. **B208**, 365 (1982).

[31] H. N. Li and S. Mishima, Phys. Rev. D **71**, 054025 (2005).